Supplementary Information

Novel skin patch combining human fibroblast-derived matrix and ciprofloxacin for infected wound healing

Muhammad Suhaeri[1,2,3,†], Mi Hee Noh[4,†], Ji-Hoi Moon[5], In Gul Kim[1], Seung Ja Oh[1], Sang Su Ha[1,6], Jong Ho Lee[1], Kwideok Park[1,6,*]

[1]Center for Biomaterials, Korea Institute of Science and Technology, Seoul 02792, Republic of Korea

[2]Unit of Education, Research, and Training, Universitas Indonesia Hospital, Universitas Indonesia, Depok 16424, Indonesia

[3]Medical Technology Research Cluster, Indonesia Medical Education and Research Institute, Faculty of Medicine, Universitas Indonesia, Jakarta Pusat 10430, Indonesia

[4]Department of Biomedical Science, Graduate School, Kyung Hee University, Seoul 02447, Republic of Korea

[5]Department of Maxillofacial Biomedical Engineering, School of Dentistry/Department of Life and Nanopharmaceutical Sciences, Kyung Hee University, Seoul 02447, Republic of Korea

[6]Division of Bio-Medical Science and Technology, KIST School, Korea University of Science and Technology (UST), Seoul 02792, Republic of Korea

†These authors contributed equally

Running title: A novel skin patch for infected wound healing

Submitted to *Theranostics*

* Correspondence: Kwideok Park, Ph.D
E-mail: kpark@kist.re.kr
Tel: +82-2-958-5288
Fax: +82-2-958-5308

July 2018

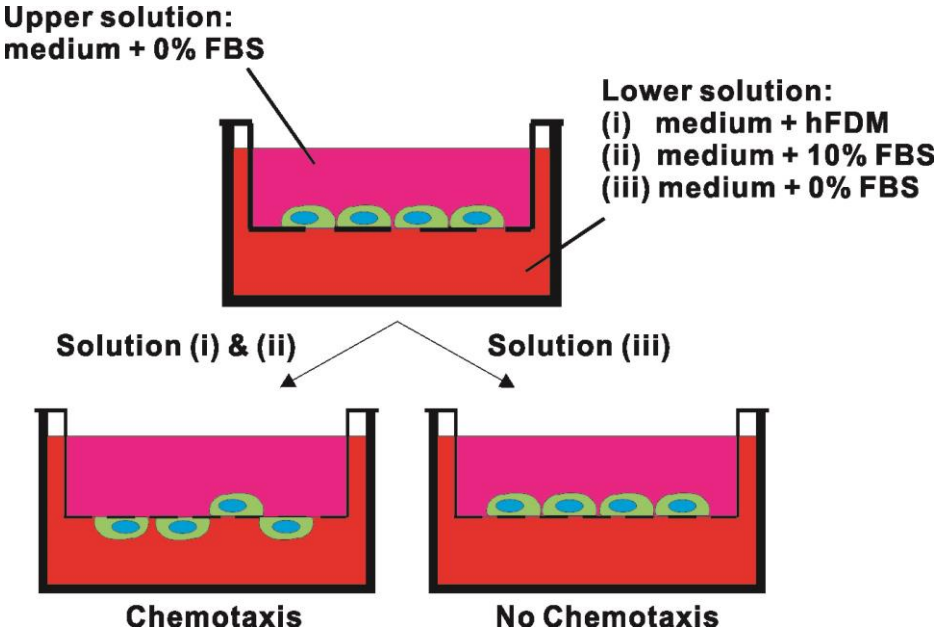

Figure S1. A schematic of experimental design of cell migration assay via a transwell system. To examine a chemotaxis effect of hFDM, three different concentrations (25, 50, and 100 μg/mL) of soluble hFDM were prepared without the addition of FBS and placed on the bottom of the chamber. For comparison study, DMEM with 10% FBS is a positive control and without serum (0% FBS) was a negative control. Two types of cells, human umbilical vein endothelial cells (HUVECs) (C2517A; Lonza) and human dermal fibroblasts (HDFs) (CRL-2522; ATCC) were used for cell migration assay.

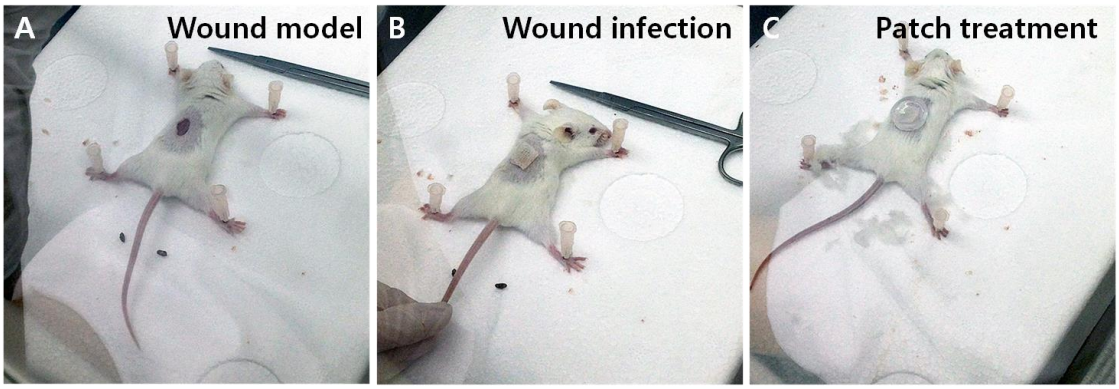

Figure S2. Images of surgical procedure for ECM patch applications into the wounded mouse model. Female 6-8 week-old BALB/c mice were used for animal experiment; A full thickness wound was prepared in the dorsal region of the mice, followed by bacterial infection of *S. aureus* into the wound area. After 6 hr post-infection, the wounds were then treated with PVA, PVA/Cipro, and PVA/Cipro/hFDM, respectively.

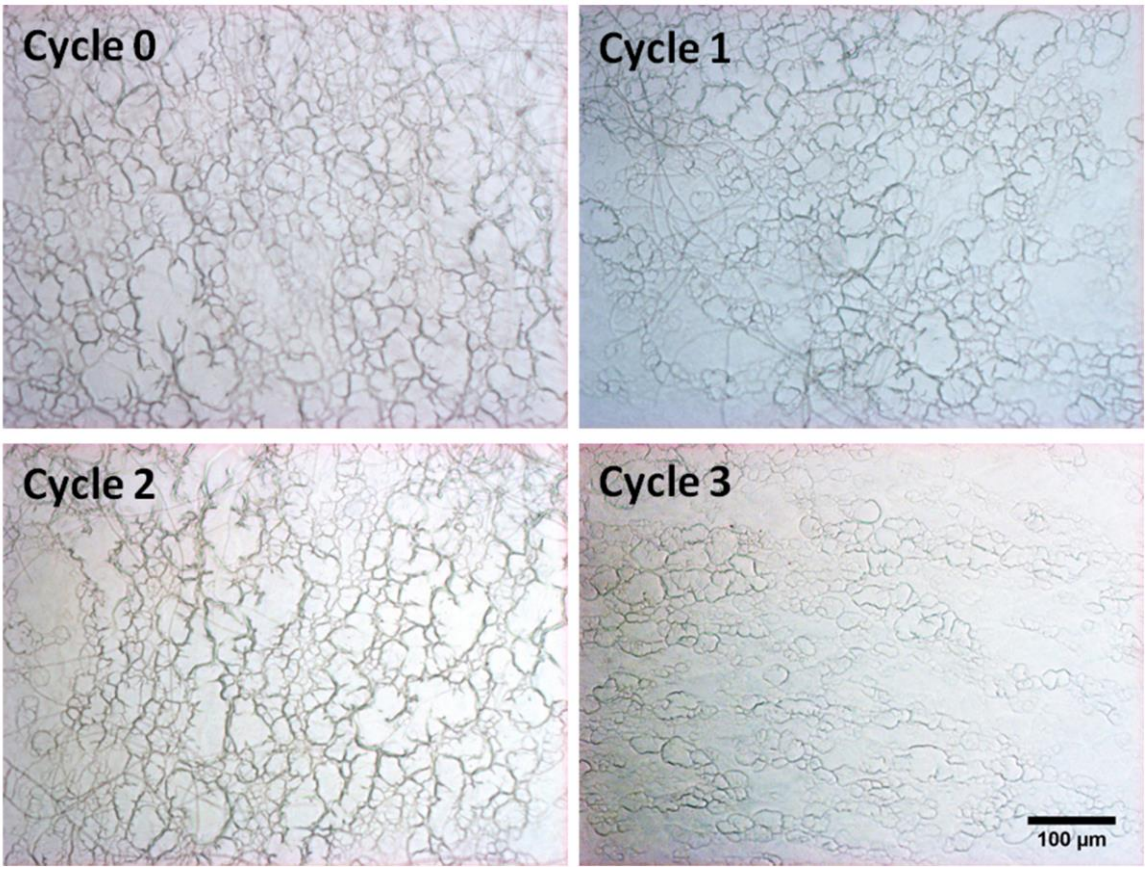

Figure S3. Examination of hFDM stability on PVA/hFDM membrane. The anchorage of hFDM to PVA hydrogel is evaluated using ultrasonication. Each cycle consists of high power ultrasonication for 5 min at 25 °C. After treatment, the persistence of fibrous hFDM structure was observed on the surface of PVA hydrogel. Scale bar is 100 μm.

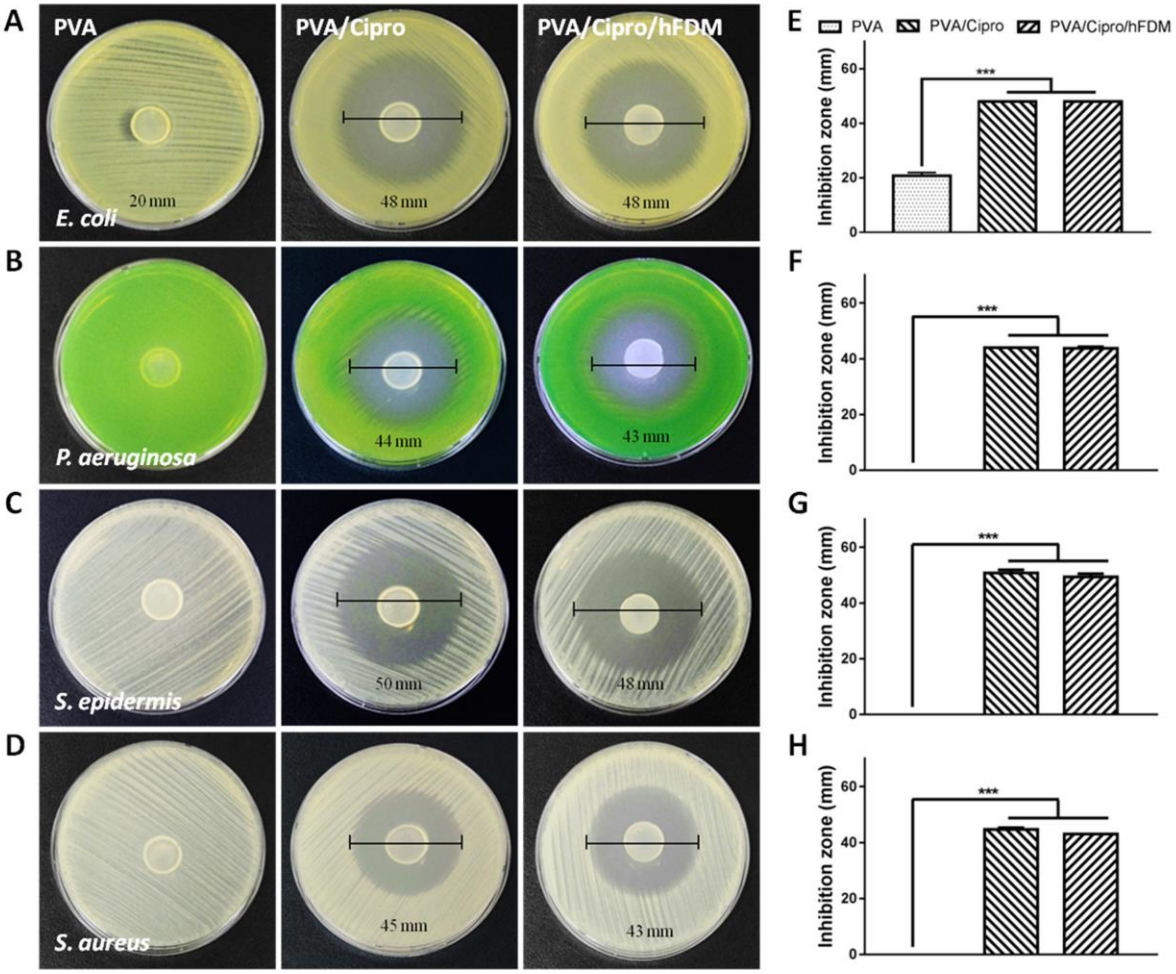

Figure S4. Antibacterial activity tests *in vitro*. (A, B, C, D) Representative images via inhibition zone assay show the antimicrobial activity of PVA, PVA/Cipro and PVA/Cipro/hFDM against gram negative (*E. coli and P. aeruginosa*) and positive (*S. epidermis and S. aureus*) bacteria. (E, F, G, H) Average diameters of inhibition zone for each bacterial strain were measured. Statistically significant difference: ***$p < 0.001$.

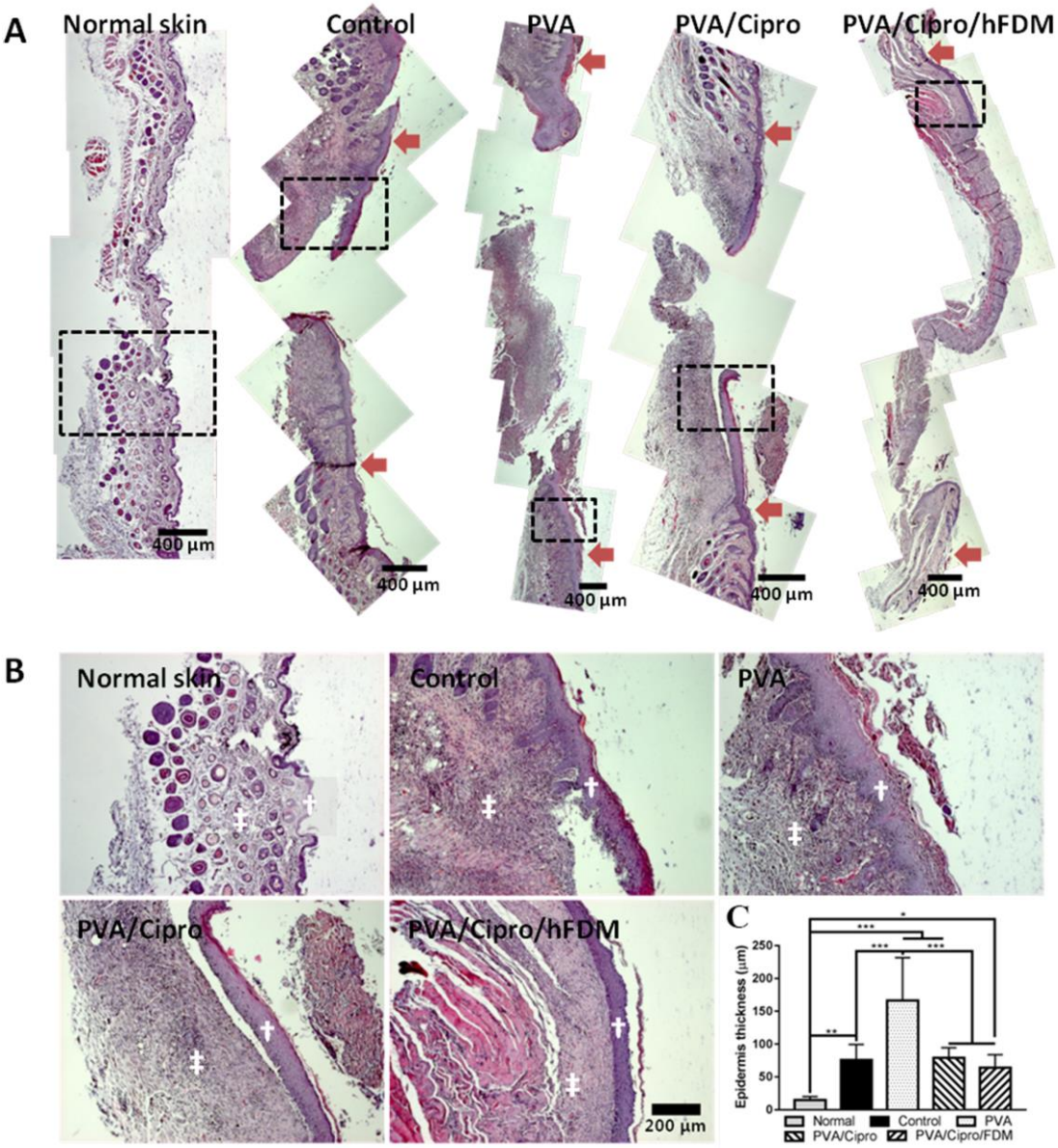

Figure S5. Analysis of dermis and epidermis regeneration on day 15. (A) Hematoxylin and eosin (H&E) staining of the skin tissues collected at 15 days post-treatments. Red arrows show the position of the initial wound areas. Dashed black boxes correspond to the area enlarged as shown in Figure S3B. Scale bars are 400 µm. (B) Higher magnification images exhibit regenerated skin tissues, where white dagger (†) and double dagger (‡) denote the epidermis and dermis layer, respectively. Scale bar is 200 µm. (C) Thickness of new epidermis. Statistically significant difference: $*p < 0.05$, $**p < 0.01$, or $***p < 0.001$.

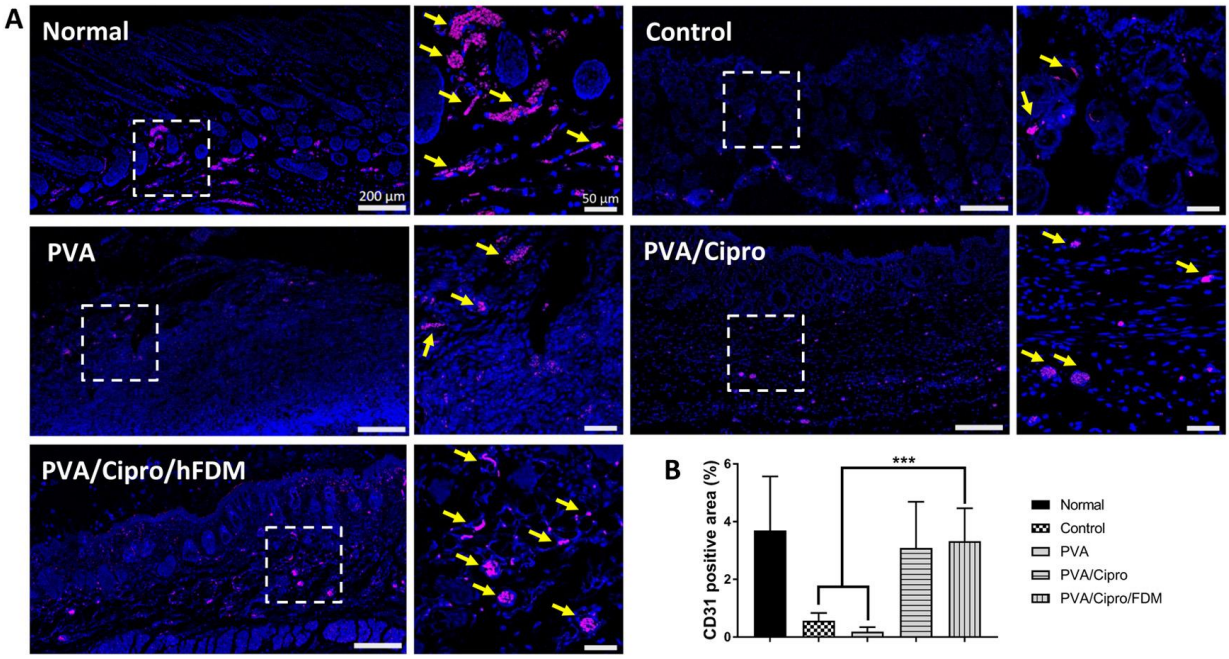

Figure S6. Immunofluorescence staining of CD31. Neovascularization was examined with tissue samples on day 21 via immunofluorescence of CD31, an endothelial cell marker. The positive signals of CD31 are marked in yellow arrows. In addition, quantitative analysis of those signals is also calculated from five random images with three replicates of each group (n = 3). Statistically significant difference: ***$p < 0.001$.

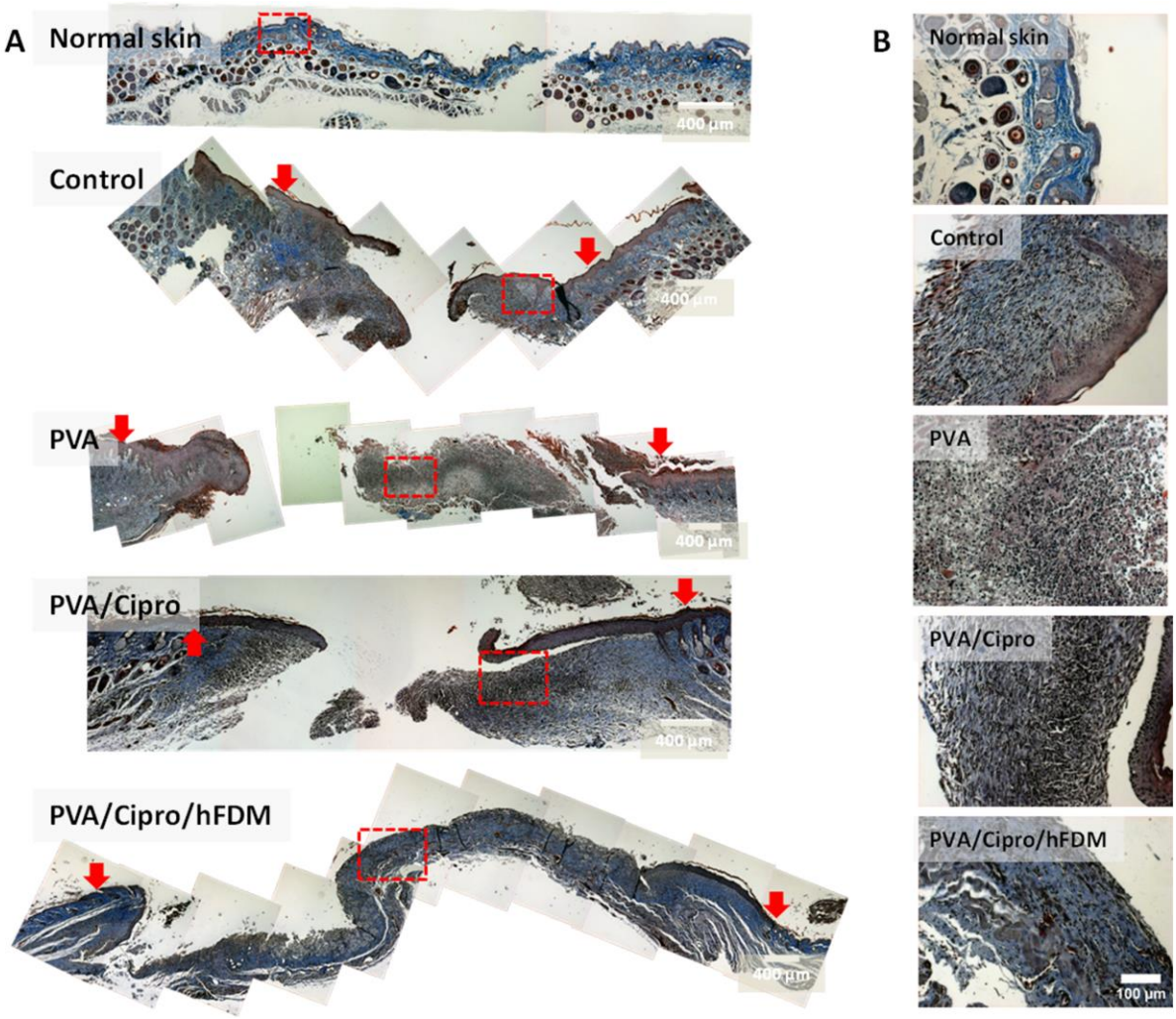

Figure S7. Analysis of collagen deposition and distribution pattern on day 15. (A) Masson's trichrome staining of the skin tissues on day 15 post-treatments. Collagen and nuclei are indicated in blue and black color, respectively. Red arrows are the position of the initial wound areas. Dashed red boxes indicate the area to be magnified. Scale bars are 400 µm. (B) Higher magnification images show deposition of collagens and their distribution pattern in the epidermis and dermis. Scale bar is 100 µm.

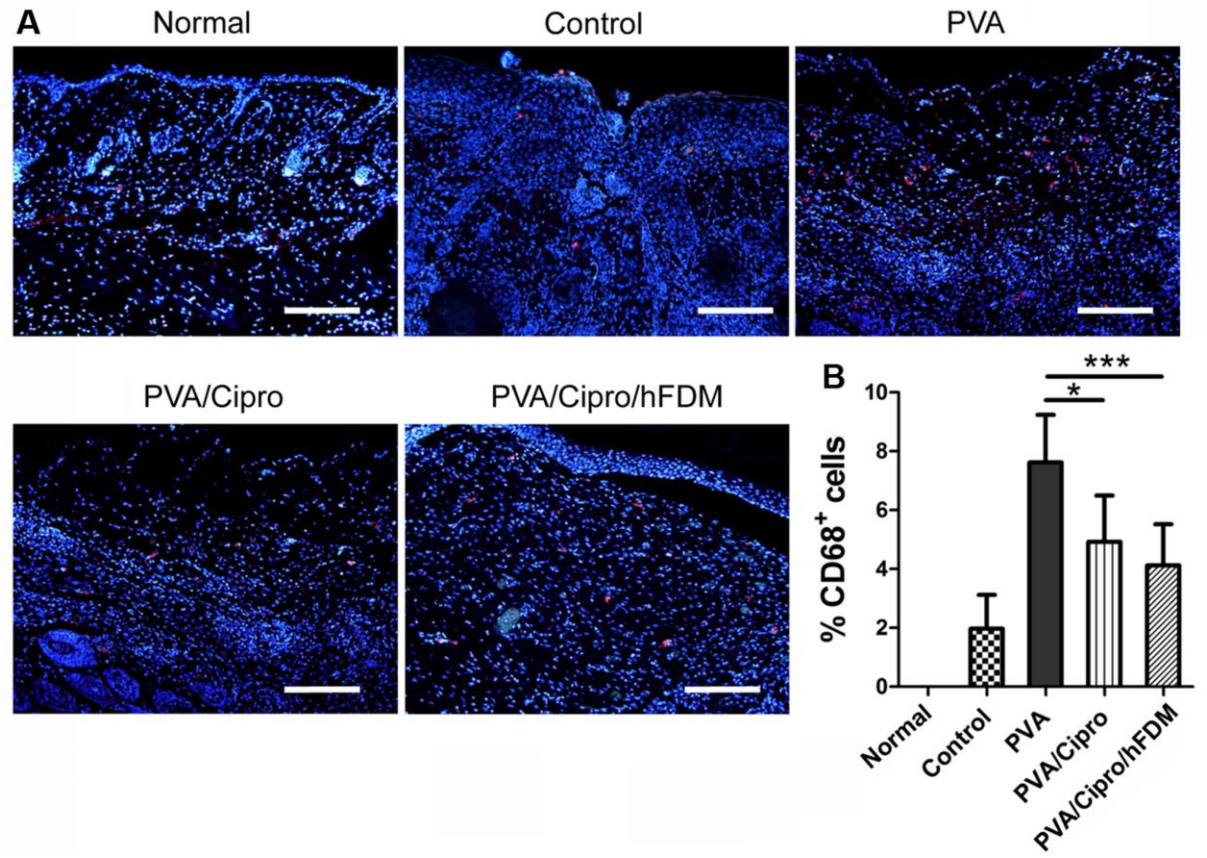

Figure S8. Macrophage (M0) population in the regenerated skin tissues on day 21. (A) Immunofluorescence of the skin tissues obtained from five test groups via macrophage (M0) marker CD68. The positive signals are detected in a pink-red color. Scale bar is 200 μm. (B) Quantitative analysis of CD68-positive signals for each group. Statistically significant difference: *$p < 0.05$ or ***$p < 0.001$.